On the Suppression of Asymmetric Artifacts Arising in an Implementation of the Thin-Wire Method of Moments

MARK A. TILSTON, MEMBER, IEEE, AND
KEITH G. BALMAIN, FELLOW, IEEE

Abstract—**The original version of the thin-wire frequency-domain moment-method program developed by Richmond has been modified to suppress the computation of nonphysical asymmetric fields. Richmond's implementation uses piecewise sinusoidal expansion and testing functions, along with filamentary current approximations. A modified version is described, termed the bridge-current version. The original program and the modified version are compared with each other and with simplified theory, where applicable, on the following symmetrical structures: a rectangular wire loop, a two-wire transmission line, and a log-periodic dipole antenna. The bridge-current version is shown to eliminate the computation of nonphysical asymmetric fields, to be essentially invariant with respect to variations in segmentation for the above structures, and to produce results that compare well with simplified theories where applicable. It is noted that the bridge-current version is particularly advantageous for structures that include close-spaced parallel wires connected by short wire segments.**

I. Introduction

A thin-wire frequency-domain moment-method program was developed by Richmond [1] to analyze antennas and scattering structures that can be modelled by interconnected wire segments. This program has been found to be very useful for a wide variety of problems in which experimental validation was employed. For example, the program has been used by Vainberg and Balmain [2] to analyze asymmetry resonances in log-periodic dipole antennas, and by Silva, Balmain, and Ford [3] to analyze the reradiation of medium frequency AM broadcast signals by steel-tower power lines.

Despite the program's usefulness, it has the defect that its results can depend on the numbering scheme of segment endpoints. In addition, it can predict asymmetrical currents in a structure whose geometry and excitation are symmetrical. Examples of the renumbering and asymmetry problems will be discussed later for a rectangular wire loop, a two-wire transmission line, and a log-periodic dipole antenna.

The program computes the mutual impedance between expansion and testing functions only for elements in the upper right triangular portion (including the main diagonal) of the moment method mutual impedance matrix. It is assumed that the mutual impedance elements are symmetrical. However, as shall be shown later, this assumption can be incorrect because of approximations in the implementation of the moment method, resulting in the renumbering and asymmetry problems mentioned above. A solution is to modify the method in order to produce truly symmetrical mutual impedance elements. This solution has the desirable features of producing reciprocity between ports on the wire structure as there should be in reality, and allowing minimal matrix inversion time and computer storage requirements because of the symmetrical matrix.

Manuscript received January 27, 1988; revised February 17, 1989. This work was supported by Bell Canada, and by Natural Sciences and Engineering Research Council of Canada Operating Grant A-4140.

M. A. Tilston was with the Department of Electrical Engineering, University of Toronto, Toronto, ON, Canada. He is now with M. A. Tilston Engineering, 90 Lawrence Avenue East, Toronto, ON, Canada M4N 1S6.

K. G. Balmain is with the Department of Electrical Engineering, University of Toronto, Toronto, ON, Canada M5S 1A4.

IEEE Log Number 8931317.

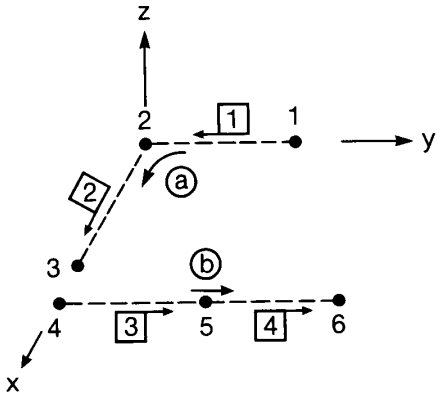

Fig. 1. Arrangement of segment axes for the example dipole-to-dipole mutual impedance problem. Boxed numbers denote monopoles, circled letters denote dipoles, unenclosed numbers denote axis point numbers. Arrows indicate reference direction for current flow.

II. Richmond's Original Program

In the concept behind the original program, the current expansion functions are set up as overlapping tubular dipolar distributions of piecewise-sinusoidal surface current. The current of an expansion dipole is axially directed, has a piecewise-sinusoidal distribution in the axial coordinate, and has no azimuthal variation. Each arm of a dipole (i.e., monopole) spans one wire segment. Each junction of N segments is the vertex of $N-1$ independent dipoles.

In Richmond's formulation, each expansion function has a corresponding testing function that spans the same length of wire, and has the same axial distribution of current, but has a different cross-sectional distribution which is filamentary along the wire axis. Because of the latter difference between an expansion function and its corresponding testing function, the mutual impedance matrix is not precisely symmetric. In other words, the reaction between a tubular expansion dipole "a" and a filamentary testing dipole "b" can differ from the reaction between the corresponding filamentary testing dipole a and tubular expansion dipole b. This asymmetry would occur, for example, in the case of two noncollinear dipoles of different lengths.

In Richmond's implementation of the above formulation, an approximation is made that can lead to an exactly symmetric mutual impedance matrix. The computation of mutual impedance between a tubular expansion dipole and a filamentary testing dipole is composed of four monopole-to-monopole mutual impedances. In the mutual impedance between an expansion monopole and a testing monopole, the tubular expansion monopole is replaced with an approximately equivalent filamentary expansion monopole. In a filamentary monopole-to-monopole mutual impedance computation, the two monopoles are placed on their respective segment axes unless the axes intersect or coincide. If the axes coincide, the monopoles are offset from each other by a wire radius in a direction orthogonal to the coincident axes. In this coincident-axis case, the equivalence between the tubular and filamentary expansion monopoles is exact because of symmetry. If the two segment axes intersect, the monopoles are offset from each other by a wire radius in a direction orthogonal to the plane containing both axes.

Fig. 1 illustrates the arrangement of segment axes in an example dipole-to-dipole mutual impedance calculation. Circled letters denote dipoles and boxed numbers denote monopoles. The unenclosed numbers denote points on the wire axis that define the span of two dipoles.

0018-926X/90/0200-0281$01.00

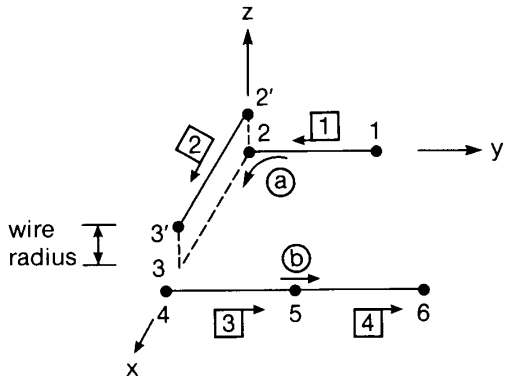

Fig. 2. Monopole locations for the example dipole-to-dipole mutual impedance problem.

Each dipole contains two monopoles. The mutual impedance between dipole a and dipole b is composed of four monopole-to-monopole mutual impedances as follows:

$$Z_{ab} = Z_{13} + Z_{14} + Z_{23} + Z_{24}$$

$$Z_{ba} = Z_{31} + Z_{32} + Z_{41} + Z_{42}.$$

Of the above pairs of monopoles, those requiring an offset are 2-3 and 2-4. Pairs 1-3 and 1-4 do not require an offset because their segment axes do not intersect. Fig. 2 shows a possible monopole geometry that satisfies the offset requirements for both Z_{ab} and Z_{ba}. The mutual impedance Z_{ab} is computed with the same current distributions as Z_{ba}, so Z_{ab} and Z_{ba} are reciprocal. Note that monopoles 1 and 2 are offset from one another, causing dipole a to be broken, while dipole b is continuous. To satisfy the continuity equation, there must be equal and opposite point charges on monopoles 1 and 2 at the dipole break. However, in the original program, the contribution of the point charge electric scalar potential gradient is not included in the **E**-field when the following mutual impedance integrals are evaluated:

$$Z_{ab} = -\int \mathbf{E}_a \cdot \mathbf{J}_b \, dV \tag{1a}$$

$$Z_{ba} = -\int \mathbf{E}_b \cdot \mathbf{J}_a \, dV \tag{1b}$$

where $\mathbf{E}_a$ and $\mathbf{E}_b$ are the electric fields of dipoles a and b, $\mathbf{J}_a$ and $\mathbf{J}_b$ are the volume current densities of dipoles a and b, unit terminal current is assumed, and the integrations cover all space. This neglect of the point charges will affect $\mathbf{E}_a$, but not $\mathbf{E}_b$ (because dipole b has no point charges). Hence, Z_{ab} will be affected, but not Z_{ba}, and reciprocity cannot hold.

To restore reciprocity to the above situation where one dipole is broken, two alternative modifications were implemented. The first involves partial inclusion of the point charge contribution to (1a), resulting in the *point-charge version* of the program. The second involves creating a bridging current in the broken dipole to flow across the break, resulting in the *bridge-current version* of the program. Although the point-charge version was found to be a good solution and has been applied successfully to the analysis of log-periodic antennas [4], the bridge-current version was found to be clearly superior, and it will be discussed in detail.

As noted earlier in this section, Richmond's formulation, if implemented exactly, would not yield a precisely symmetric mutual impedance matrix. However, the approximate implementation, which involves only filamentary currents, leads to an exactly symmetric matrix provided that broken dipoles are handled carefully. Because the approximation is symmetric, the authors prefer to view it as representing a formulation that is also symmetric. The preferred symmetric formulation is one in which each tubular expansion function has a corresponding identical tubular testing function.

III. Bridge-Current Version

In Section II it was shown that a broken dipole can arise in the original program. In the bridge-current version, a new current is introduced to bridge any break in a dipole. For example in Fig. 2, a bridge current would flow from point 2 to 2'. For simplicity, the bridge current is chosen to be a constant across the break. To facilitate programming, the mutual impedance integral (1a) is rearranged into a symmetric form. This is done by first expressing the **E**-field in (1a) terms of the electric scalar potential gradient and the magnetic vector potential, then integrating the term containing the electric scalar potential gradient by parts, and finally utilizing the continuity equation to obtain the following result:

$$Z_{ab} = j\omega \iint \left[\frac{\mu}{4\pi} \mathbf{J}_a(\mathbf{r}') \cdot \mathbf{J}_b(\mathbf{r}) + \frac{1}{4\pi\epsilon} \rho_a(\mathbf{r}')\rho_b(\mathbf{r}) \right] \frac{e^{-\gamma R}}{R} \, dV \, dV' \tag{2a}$$

where

$$R = |\mathbf{r} - \mathbf{r}'|, \tag{2b}$$

and ρ_a and ρ_b are the volume charge densities of dipoles a and b. From (2a) it is clear that Z_{ab} and Z_{ba} are equal. It is noted that, for short separations, the first term is related to inductive coupling and the second term is related to capacitive coupling.

Consider the application of (2a) to the dipoles shown in Fig. 2, with an added bridge current bridging the break in dipole a. Because the bridge current is orthogonal to dipole b, the dot product of the bridge-current part of $\mathbf{J}_a$ and $\mathbf{J}_b$ is zero, and the bridge current does not contribute to the first term of (2a). Because the distribution of the bridge current is constant, it has no associated distributed charge, and continuity of current guarantees no end charges, so the bridge current does not contribute to the second term of (2a). Hence the bridge current makes no contribution to (2a), and can thus be ignored when computing Z_{ab}. Note that the same mutual impedance Z_{ab} would be obtained using (1a), although the bridge current would have to be included in the computation.

Because the bridge current can be ignored when using (2a), the only change required to the original program is to evaluate the mutual impedance between monopoles using (2a) instead of (1a), using only the *distributed* charge on the monopoles. This requires that changes be made only to subroutine GGMM.

The specific modifications will now be described utilizing Richmond's terminology where possible. They are specific to subroutine GGMM. Fig. 3 shows two filamentary monopoles of which monopole s spans points s_1 and s_2, and monopole t spans points t_1 and t_2. The current distributions are as follows:

On monopole s,

$$\mathbf{I}_i(s) = \hat{\mathbf{s}} \frac{\sinh \gamma(s - s_k)}{\sinh \gamma(s_i - s_k)} \tag{3}$$

where $i = 1$ or 2, $k = 2/i$ and $s_1 \le s \le s_2$.

On monopole t,

$$\mathbf{I}_j(t) = \hat{\mathbf{t}} \frac{\sinh \gamma(t - t_l)}{\sinh \gamma(t_j - t_l)} \tag{4}$$

where $j = 1$ or 2, $l = 2/j$ and $t_1 \le t \le t_2$. Utilizing (2a), the mutual impedance between monopoles s and t is

$$Z_{st}^{ij} = j\omega \int_{t_1}^{t_2} \int_{s_1}^{s_2} \left[\frac{\mu}{4\pi} I_i(s) I_j(t) \cos\psi + \frac{1}{4\pi\epsilon} q_i(s) q_j(t) \right] \frac{e^{-\gamma R}}{R} \, ds \, dt \quad (5)$$

where $R = [s^2 + t^2 - 2st\cos\psi + d^2]^{1/2}$ and $d > 0$.

Applying the continuity equation to (3) and (4) gives q_i and q_j. Substituting the current and charge distributions into (5) yields

$$Z_{st}^{ij} = C'_{ij} \int_{t_1}^{t_2} \int_{s_1}^{s_2} [\sinh\gamma(s - s_k)\sinh\gamma(t - t_l)\cos\Psi + \cosh\gamma(s - s_k)\cosh\gamma(t - t_l)] \frac{e^{-\gamma R}}{R} \, ds \, dt$$

where

$$C'_{ij} = \frac{j\omega\mu}{4\pi \sinh\gamma(s_i - s_k)\sinh\gamma(t_j - t_l)}.$$

Expanding the sinh and cosh functions in terms of exponential functions yields

$$Z_{st}^{ij} = C_{ij} \sum_{p=1}^{2} \sum_{q=1}^{2} e^{-\gamma(ms_k + nt_l)} mn I_{pq} \quad (6a)$$

where

$$C_{ij} = \frac{\eta}{16\pi \sinh\gamma(s_i - s_k)\sinh\gamma(t_j - t_l)}, \quad (6b)$$

$$\eta = \sqrt{\mu/\epsilon}, \quad m = (-1)^{p-1}, \quad n = (-1)^{q-1}, \quad (6c)$$

and

$$I_{pq} = \gamma \frac{1 + mn\cos\psi}{mn} \int_{t_1}^{t_2} \int_{s_1}^{s_2} \frac{e^{\gamma(ms + nt - R)}}{R} \, ds \, dt. \quad (6d)$$

The integral I_{pq} has been evaluated in terms of exponential integrals as shown in the following:

$$I_{pq} = \sum_{h=1}^{2} (-1)^h \left[-e^{\gamma t_h (n + m\cos\psi)} \int_{v(s_1, t_h)}^{v(s_2, t_h)} \frac{e^{-z}}{z} \, dz - e^{\gamma s_h (m + n\cos\psi)} \int_{w(s_h, t_1)}^{w(s_h, t_2)} \frac{e^{-z}}{z} \, dz + e^{\gamma j u_0} \int_{x(s_h, t_1)}^{x(s_h, t_2)} \frac{e^{-z}}{z} \, dz + e^{-\gamma j u_0} \int_{y(s_h, t_1)}^{y(s_h, t_2)} \frac{e^{-z}}{z} \, dz \right] \quad (7)$$

where

$$v(s, t) = \gamma(-ms + mt\cos\psi + R),$$
$$w(s, t) = \gamma(-nt + ns\cos\psi + R),$$
$$x(s, t) = \gamma(-ms - nt + R + ju_0),$$
$$y(s, t) = \gamma(-ms - nt + R - ju_0),$$

and

$$u_0 = d \left[\frac{1 + mn\cos\psi}{1 - mn\cos\psi} \right]^{1/2}.$$

Note that each integration variable is a complex constant multiplied by a real function which is sometimes added to an imaginary constant.

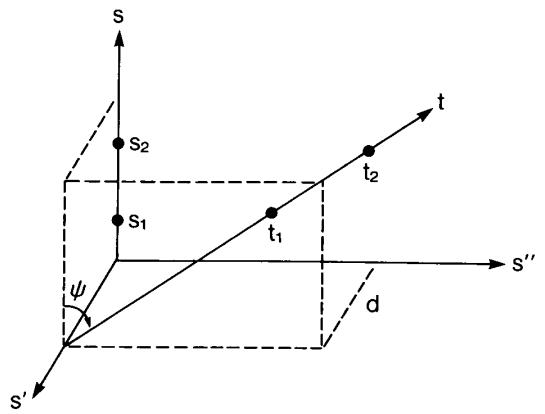

Fig. 3. Coordinate system used to analyze the mutual impedance between two monopoles.

The integration path is therefore a straight line on the complex plane. The function

$$w_{12}(z_1, z_2) = \int_{z_1}^{z_2} \frac{e^{-z}}{z} \, dz \quad (8)$$

for straight line path is evaluated in subroutine EXPJ in the original program.

Limiting cases occur when the monopoles are parallel, causing u_0 to be zero or infinite. u_0 becomes zero when $1 + mn\cos\psi$ is zero. In this case, it can be shown that $I_{pq} = 0$. u_0 becomes infinite when $1 - mn\cos\psi$ is zero. In this case, it can be shown that the last two terms of I_{pq} in (7) vanish.

IV. Comparative Results of the Two Program Versions

Computations using the original program and the bridge-current version have been compared with one another for a rectangular wire loop, a two-wire transmission line, and a log-periodic dipole antenna. For the rectangular loop and the transmission line, the computations were also compared with simplified theory. The computations were done on a microcomputer having an 8088 microprocessor (eight-bit) with an 8087 math coprocessor, using standard Fortran 77. For complex numbers and functions, single precision (i.e., COMPLEX*8) was used except where otherwise noted.

A. Rectangular Loop

The two versions were used to compute the input impedance of a rectangular loop of perfectly conducting wire whose dimensions were 30 by 7.5 mm. The wire had a radius of 1.25 mm and had infinite conductivity. The frequency was 100 MHz. Note that the wire on the short side has a length-to-radius ratio of only six, whereas a ratio of ten or more is often preferred to avoid numerical errors in thin-wire computations. Because this loop is electrically small, i.e., only 0.025 λ in perimeter, the input reactance can be computed approximately using an inductance formula. Such a formula is given by the U.S. National Bureau of Standards [5], as follows:

$$L = \frac{\mu}{\pi} \left[(l_1 + l_2) \ln \frac{2l_1 l_2}{a} - l_1 \ln(l_1 + l_d) - l_2 \ln(l_2 + l_d) + 2(l_d + a - l_1 - l_2) \right] \quad (9)$$

where the formula has been converted for units of m, H, and natural logarithms; l_1, l_2, and l_d are the length, width and diagonal dimensions of the rectangle, and a is the wire radius. Using this formula,

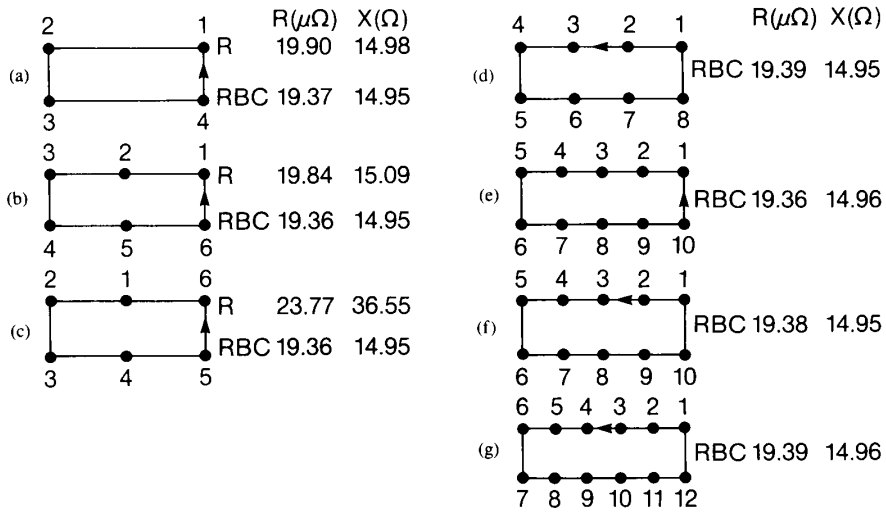

Fig. 4. Impedance of a perfectly conducting rectangular wire loop computed by the original Richmond program (R) and the bridge current version (RBC) of the program. All computations used double-precision complex numbers and functions. Dots denote segment end points, and arrows denote voltage generators. Voltage generators are located at the segment end at which the arrow points. The impedance obtained from simplified theory is $19.52 \times 10^{-6} + j14.94\ \Omega$.

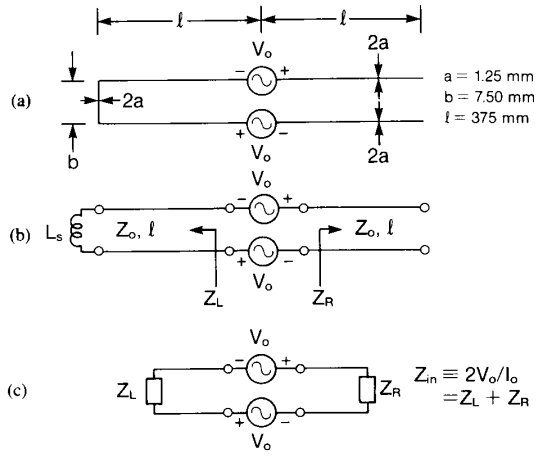

Fig. 5. Resonant quarter-wave stub. (a) Dimensions and feed details. (b) Equivalent transmission-line circuit. (c) Equivalent lumped-element circuit.

the loop inductance is 0.02377 μH, which has a reactance of 14.94 Ω at 100 MHz.

The radiation resistance was computed by means of numerical integration of the radiated power flowing through a spherical surface in the far-field region. A resistance of 19.52 $\mu\Omega$ was obtained.

Fig. 4 shows various segmentations and corresponding impedances computed with the original program (R) and the bridge-current version (RBC). For complex numbers and functions, double precision was required in order to obtain accurate resistances. It can be seen that the bridge-current version is very stable, consistently yielding a resistance in the range of 19.36 to 19.39 $\mu\Omega$, and yielding a reactance of 14.95 or 14.96 Ω. These results are very close to the impedance of $19.52 \times 10^{-6} + j14.94\ \Omega$ obtained from the simplified theory. Comparing Figs. 4(b) and 4(c), one sees that the original program predicts reactances that change from 15.09 to 36.55 Ω and resistances that change from 19.84 to 23.77 $\mu\Omega$, solely because the point numbering scheme was changed.

B. Resonant Quarter-Wave Stub

The input reactance was computed, using transmission line theory and the moment method, for the two-wire transmission line stub shown in Fig. 5(a). The line has a width of 7.5 mm and a length of 750 mm which is 0.25017 λ at the test frequency of 100 MHz. The transmission line is short circuited at one end, and open circuited at the other. The radius of the wire for both the transmission line and the short circuit is 1.25 mm, and the conductivity is infinite. As with the rectangular loop example, the short-circuiting wire has a length-to-radius ratio of only six.

Fig. 5(b) shows the equivalent transmission line circuit. The characteristic impedance Z_0 of the transmission line is 211.53 Ω. The self inductance L_s of the short-circuiting wire is approximately the same as the mutual inductance of two parallel filamentary currents spaced a wire radius apart. It was computed to be 2.4669×10^{-9} H, which yields a reactance of 1.55 Ω at 100 MHz. The resulting transmission line theory input reactance as defined in Fig. 5(c) is 3.57 Ω.

Fig. 6 shows the moment method predicted reactances for various segmentations. Note that in the first segmentation, the length ratio of adjacent segments at the corner junction is 50:1. A large length ratio such as this could conceivably lead to inaccurate results, but no problem with the RBC version arises in this computation or in other comparable ones. The original program (R) is seen to predict reactances that vary with the numbering scheme of the segment end points, introducing errors that vary with segmentation, the worst case being Fig. 6(f) with an order-of-magnitude error. However, for any segmentation, there is one numbering scheme that produces predicted reactances that agree well with transmission line theory. The bridge-current (RBC) version is insensitive to the point numbering scheme and the segmentation, yielding reactances between 3.55 and 3.65 Ω, which is in good agreement with the transmission-line-theory computation.

C. Log-Periodic Dipole Antenna

A log-periodic dipole antenna (LDPA) analysis has been done by Vainberg and Balmain [2] using Richmond's original program. They computed asymmetry resonances produced on LPDAs in which the

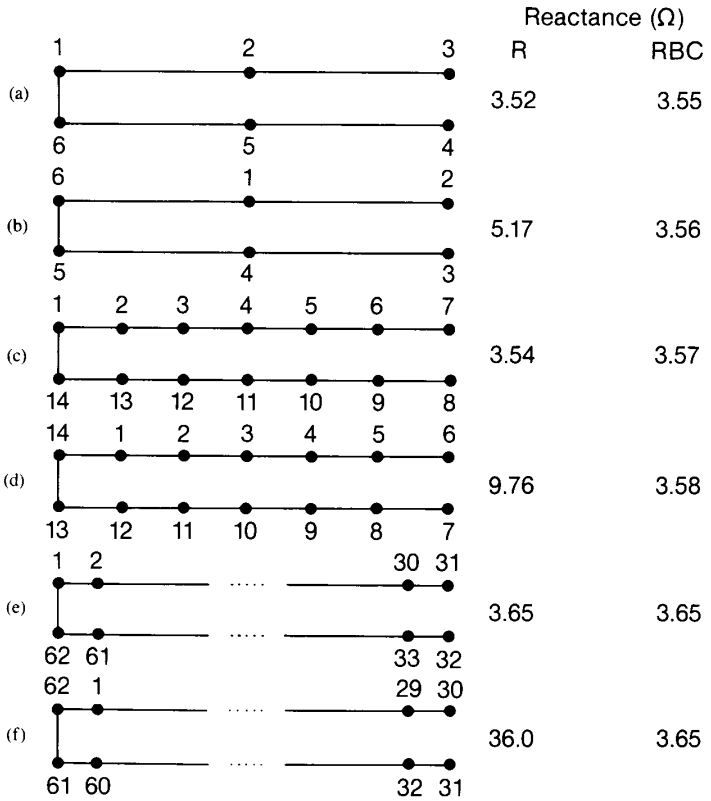

Fig. 6. Reactance of quarter-wave stub at 100 MHz computed by R and RBC moment methods. Dots denote segment end points. The stub dimensions and feed details are shown in Fig. 5(a), where $l = 375$ mm, $b = 7.5$ mm, and $a = 1.25$ mm. The wire is assumed to be perfectly conducting. The reactance obtained from transmission-line theory is 3.57 Ω.

symmetry was destroyed by an extension of one of the monopoles on the antennas. One surprising result was that, in the case of a perfectly symmetric antenna, the program still predicted asymmetry resonances, four of them in the case studied. For a symmetric antenna, the currents on the two feeder wires should be equal and opposite everywhere. Hence, to either side of the antenna, the far E-field polarized parallel to the feeder wires should be zero. A measure of the "computer generated asymmetry," therefore, is the side radiation, relative to the radiation on the antenna boresight. Vainberg and Balmain found that, with the original program, the side radiation exhibited peaks at four frequencies with maxima 50 dB below the boresight radiation, a level much too high to be attributed to computer round-off errors. They noted that a different segmentation using only one segment per monopole instead of two segments produced side radiation of 110 dB below the boresight radiation. In the present work, the above analysis using two segments per monopole was repeated using the bridge-current version. The predicted side radiation versus frequency was plotted, and four rather ill-defined peaks were identified, the highest levels of these peaks being at least 110 dB below the boresight radiation.

V. Conclusion

A modified version of Richmond's original thin-wire program has been presented, namely the bridge-current version. This version has been shown to be insensitive to both the model segmentation scheme and the point numbering scheme, in contrast to the original program which could generate impedance values in error by as much as an order of magnitude. The bridge current version is also in good agreement with magnetostatic theory for the small rectangular wire loop, and with transmission line theory for the two-wire quarter-wave stub. Both the rectangular loop and the stub are relevant to the analysis of complicated wire antennas such as the log-periodic dipole antenna which involve close-spaced parallel wires in both the feeder structure and the radiating elements. The bridge-current version applied to log-periodic antennas suppresses non-physical asymmetric side radiation from symmetric structures to the point where true asymmetry resonances caused by perturbations in antenna geometry can be analyzed with confidence. Therefore, it is expected that this version of the program should be particularly useful in the analysis of other antennas that incorporate either parallel feed wires or parallel-wire stubs.

References

[1] J. H. Richmond, "Radiation and scattering by thin-wire structures in a homogeneous conducting medium," *IEEE Trans. Antennas Propagat.*, vol. AP-22, no. 2, p. 365, Mar. 1974. (Computer code available in: J. H. Richmond, "Computer program for thin wire structures in a homogeneous conductive medium," National Technical Information Service, Springfield, VA 22151, NASA CR-2399, June 1974.)

[2] M. Vainberg and K. G. Balmain, "On prediction of the asymmetry resonance phenomenon of log-periodic dipole antennas," *Can. Elec. Eng. J.*, vol. 6, no. 3, pp. 31–34, July 1981.

[3] M. M. Silva, K. G. Balmain, and E. T. Ford, "Effects of power line reradiation on the patterns of a dual frequency MF antenna," *IEEE Trans. Broadcasting*, vol. BC-28, no. 3, pp. 94–103, Sept. 1982.

[4] M. Hilbert, M. A. Tilston, and K. G. Balmain, "Resonance phenomena of log-periodic antennas: characteristic-mode analysis," *IEEE Trans. Antennas Propagat.*, vol. 37, no. 10, pp. 1224–1234, Oct. 1989.

[5] U.S. National Bureau of Standards, "Radio instruments and measurements," Circular 74, Mar. 10, 1924, eq. 138.